Shaping Arbitrary Energy Landscapes with Feedback

by Avinash Kumar[1] and John Bechhoefer

Avinash Kumar
<aka106@sfu.a>,
John Bechhoefer
<johnb@sfu.ca>

Dept. of Physics,
Simon Fraser
University, 8888
University Dr.,
Burnaby, BC
V5A 1S6

The interaction of light with matter at the nanoscale has been a topic of great importance over the past several decades. After pioneering work by Ashkin *et al*. [1], optical tweezers have been used to exert forces on small mesoscopic particles as well as to detect their fluctuations for physical [2,3], chemical [4,5], and biological applications [6-8]. Other forms of tweezers use forces based on optofluidics [9], plasmonics [10], and photophoresis [11].

In addition to passive traps that create potential wells to confine particles, there are traps that create *virtual potentials* that confine particles using active feedback based on position measurements of the trapped object. Such feedback traps need only create a force of controlled magnitude and direction and apply confinement based on feedback from position measurements. The feedback trap can be based on a variety of forces, including electrokinetics [12], magnetism [13], and thermophoresis [14]. Sometimes the goal is to apply a more complicated force field rather than just creating a trap [15]. Feedback traps based on optical tweezers [16] use forces from the underlying harmonic potential to achieve such goals. In this article, we explore the idea that using feedback based on the measured particle position, one can create essentially arbitrary potentials.

Typically, an optical tweezer uses a tightly focused Gaussian beam to trap microspheres. In our experiment, we trap 1.5 μm diameter silica beads. A particle in a trap can be modelled as a dielectric particle placed in an inhomogeneous electric field. Forces acting on the particle from the external field are categorised into scattering and gradient forces. *Scattering forces* arise from momentum transfer from photons to particle and push the particle along the direction of propagation of the light. *Gradient forces* arise from gradients in the electric field and act in the direction of increasing electric field. If the total gradient force exceeds the scattering force, a particle is trapped.

Summary

A closed-loop feedback trap based on optical tweezers enables the shaping of arbitrary energy landscapes for colloidal particles.

Since an optical tweezer exerts a force to counteract fluctuations, it can be used to provide feedback forces on colloidal particles to probe and manipulate their dynamics with high resolution and bandwidth.

Here, we combine the technique of optical tweezers with feedback control to create virtual potentials by applying varying forces on a particle. The feedback protocolinvolves observation of the position of a freely diffusing particle, calculation of a force based on an imposed potential and application of that force (Fig. 1). Optical tweezers have previously used feedback to create position and force clamps [17-19]. In a force clamp, feedback is used to apply a constant force on the trapped particle. In a position clamp, the forces are varied to keep a particle at a desired position. In our version of feedback trap, we update force and position at rates of order 100 kHz to create a virtual energy landscape. It should be noted that these virtual potentials are discrete approximations of real potentials. In a real potential, forces are applied instantaneously as the position changes, but in a virtual potential, feedback forces are set once per feedback loop and are approximately constant throughout the loop. The performance of a feedback trap is limited by the amount of latency (delay) in the control system.

Our feedback optical tweezer is based on a homemade microscope. A water-immersion high-numerical-aperture microscope objective (60X, NA = 1.2) is used for trapping. A low-numerical-aperture microscope objective (20X, NA = 0.4) focuses the detection laser on the trapped particle to detect the fluctuations. The trap centre is shifted regularly to create a feedback force. This is done by an acoustooptic deflector which is imaged on the back focal plane of the trapping objective. Angular deviation of the deflector output is translated into a linear shift in the trapping plane. A quadrant photodiode detector is used to read the signals from the trapped particle. In order to precisely apply the feedback forces, the feedback timing should be accurate. We use a National Instruments FPGA-based data acquisition module (NI USB-7855R) that runs at a deterministic time step of 10 μs and can read and write signals simultaneously. The setup is described in more detail in Ref. [16].

1. Avinash Kumar received 2nd place in the CAP Best Student Poster Presentation competition at the 2019 CAP Congress at Simon Fraser University in Burnaby, BC.

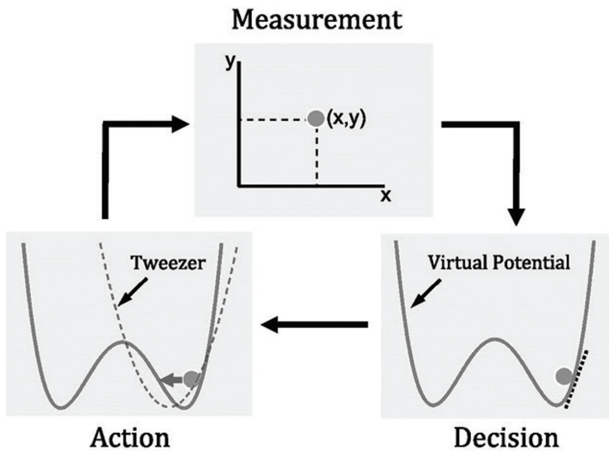

Fig. 1 One cycle of a feedback trap. *Measurement*: estimate the current position of the particle, *Decision*: calculate force based on the imposed potential (red), and *Action*: apply the force by shifting the harmonic well centre (blue).

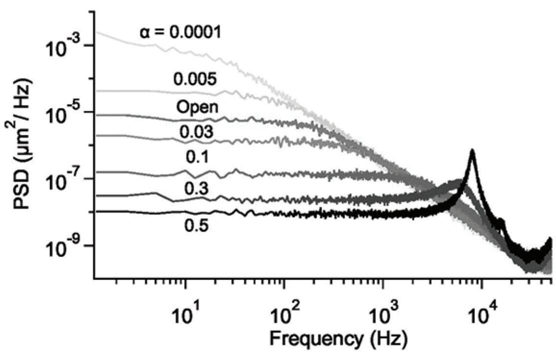

Fig. 2 Power spectral density for different feedback gains. The red plot corresponds to the "open loop" optical tweezer (no feedback). The other curves correspond to different feedback gains. Feedback can create both stiffer and weaker traps.

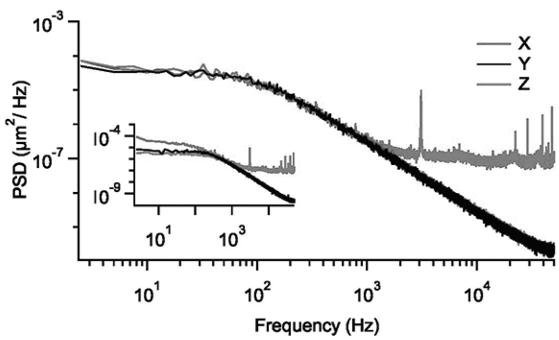

Fig. 3 Power spectral density in x, y and z directions. Inset: power spectrum density without feedback. With x and y feedback, all three dimensions show the same stiffness.

Using feedback, we create virtual harmonic wells of variable stiffness [16]. A similar instrument has been developed independently by Albay *et al*. [20]. The discrete dynamics of a particle in a virtual harmonic well is given as

$$x_{n+1} = x_n - \tilde{\alpha}\,(x_n - x_n^t) + \xi_n \tag{1a}$$

$$x_n^t = \bar{x}_n(1-G) \tag{1b}$$

$$\bar{x}_n = x_{n-2} + \zeta_n, \tag{1c}$$

where x_n is the particle's real position, $\bar{x}_n$ the observed positions, x_n^t the trap position at time t_n, ξ_n the integrated thermal noise, ζ_n the integrated measurement noise, and $G \equiv k_v/k_t$ is a dimensionless gain. Here, k_v is the stiffness of the virtual trap and k_t that of the real trap. The constant $\tilde{\alpha} = G[1 - \exp(\Delta t/t_r)]$ accounts for the relaxation in the trap during one cycle of the feedback loop, Δt. Here, $t_r = \gamma/k_t$ is the relaxation time, γ the viscous drag coefficient. We operate our trap in the limit $\Delta t << t_r$ where $\tilde{\alpha} \approx \alpha \equiv \Delta t/t_r$. The feedback delay time is $t_d = 20\ \mu s = 2\Delta t$.

Figure 2 shows that we can change the effective stiffness of a virtual trap using feedback at constant laser power. We obtained a 30-fold gain in the stiffness of the trap compared to that of the underlying harmonic trap. Often changes in trap stiffness are created by varying the total laser intensity in the trap. In a feedback trap, a similar control is achieved by changing the feedback gain α. For large values of α, the particle dynamics deviates from potential motion, showing oscillations and even instability because of overcorrection [21]. We work with α values where the variance is minimum.

Another interesting feature of a feedback trap is its ability to *reduce* trap strength [16]. In an ordinary optical tweezer, the axial stiffness is weaker than the transverse stiffness. See the inset in Fig. 3. This asymmetry is an inherent feature of the electric-field gradient of a Gaussian beam. Figure 3 shows that the usual anisotropic trap can be made isotropic in all three dimensions using feedback. We used the feedback to reduce the trapping strength in the transverse directions so that it matches the axial stiffness. Isotropy is an important property, as it allows a force sensor to measure three-dimensional forces in a straightforward manner. In an anisotropic trap, one would have to allow for different bandwidths in different directions, which complicates the interpretation of force measurements.

To demonstrate the flexibility of our feedback trap, we create a variety of virtual potentials such as harmonic well, double-well and linear potentials (Fig. 4). In Ref. [16], we have shown a family of double-well potentials where the barrier height, well separation and the curvatures are controlled independently. Note that for a linear potential, the curvature at the centre is

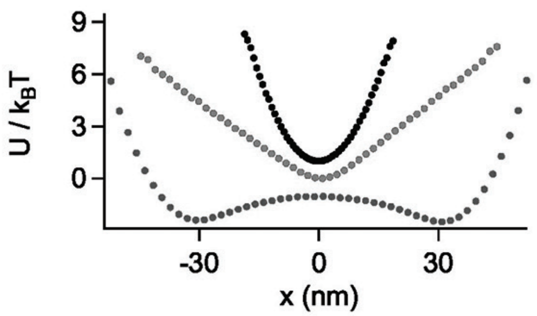

Fig. 4 A family of virtual potentials $U(x)$ showing harmonic (star), linear (triangle) and a double-well shapes (square). The potentials are reconstructed from the corresponding Boltzmann distribution of the position measurements. The three cases are offset by k_BT to aid in visualization.

governed by the feedback time and the force exerted, F. The basin at the centre can be approximated by a harmonic well with $\alpha = \frac{F}{\gamma}\Delta t/\Delta x$, where Δx is the range over which the harmonic approximation holds.

Other methods such as time-shared optical tweezers and holographic tweezers can create such energy shapes. Nanometer-scale precision in displacements can be achieved with holographic tweezers [22], but the spatial scale of the potential minima will be diffraction limited. If the goal is simply to create a double-well potential, timeshared traps are useful. However, in such traps, the effective stiffness per well becomes smaller as well separation is reduced. Well separation and barrier height are coupled, too. Here, we can *independently* vary well separation, well curvature, and barrier height [16].

In Ref. [16], we reduced the length scale of these one dimensional double-well potentials to a well spacing of 10.6 nm with a barrier height of $0.16k_BT$ [16]. These length scales are far below the diffraction limit and cannot be created with techniques such as multiplexed or holographic tweezers. The ability to create a double-well potential with low energy barrier but high well curvature is important, as it traps the particle in a well-defined volume of space while still allowing for fast transitions between macrostates.

Currently we are using our tweezer-based feedback trap to explore the *Mpemba effect* and its inverse. As described by the Tanzanian high-school student Erasto Mpemba in 1969, when two identical water samples are prepared initially at hot and warm temperatures and then quenched to a cold temperature, the hot system can cool (and freeze) faster than the warm one—a phenomenon now known as the Mpemba effect [23]. The cooling anomaly has been predicted theoretically in other systems such as nanotube resonators [24], spin glasses [25], and experimentally observed in clathrate hydrates [26]. Many explanations have been proposed, involving processes such as evaporation [27], convection [28], supercooling [29], dissolved gases [30], and hydrogen bonding [31]. These hypothetical mechanisms all have at least some experimental support, suggesting that multiple factors can lead to the anomalous cooling of the Mpemba effect. Indeed, the problem with traditional approaches is that there can be *too many* explanations, implying that they miss essential aspects of the phenomena.

Our approach to the Mpemba effect is based on a recent study by Lu and Raz [32], who argued that the Mpemba effect can be seen (and hence better understood) in a much simpler context (Brownian particle in a potential) and that the simplicity of such situations can clarify the mechanisms behind the effect. In preliminary work [33], we have explored cooling and heating in a tilted double-well potential with asymmetric domains. If the asymmetry is chosen to give a direct path between high- and low-temperature basins of attraction, we observe that an initial hot state cools to the bath temperature faster than an initially warm state [33].

In summary, we have created virtual harmonic wells and static double-well potentials with feedback. The form of such potentials can be arbitrary and are easily tunable. Virtual double-well potentials have been used previously to test the fundamental relationship between information and thermodynamics [34,35]. Experimental studies reveal that biological processes such as protein folding occurs at scales which can be described by the diffusive dynamics in a low-energy landscape [36]. The virtual potentials described here will be useful for such studies.

ACKNOWLEDGEMENTS

This research has been supported by Discovery and RTI Grants from the National Sciences and Engineering Research Council of Canada (NSERC).

REFERENCES

1. A. Ashkin, J. Dziedzic, J. Bjorkholm, and S. Chu, "Observation of a single-beam gradient force optical trap for dielectric particles," *Opt. Lett.* **11**, 288-290 (1986).
2. J. Liphardt, S. Dumont, S.B. Smith, I. Tinoco, and Bustamante, "Equilibrium information from nonequilibrium measurements in an experimental test of jarzynski's equality," *Science*, **296**, 1832-1835 (2002).

3. A. Bérut, A. Arakelyan, A. Petrosyan, S. Ciliberto, R. Dillenschneider, and E. Lutz, “Experimental verification of Landauer’s principle linking information and thermodynamics,” *Nature*, **483**, 187 (2012).
4. H. Yao, H. Ikeda, Y. Inoue, and N. Kitamura, “Optical control of fusion of microparticles in solution and simultaneous spectrophotometric measurements,” *Anal. Chem.* **68**, 4304-4307 (1996).
5. K. Ajito and K. Torimitsu, “Single nanoparticle trapping using a raman tweezers microscope,” *Appl. Spectrosc*, **56**, 541-544 (2002).
6. A. Ashkin and J. Dziedzic, “Internal cell manipulation using infrared laser traps,” *Proc. Natl. Acad. Sci.* **86**, 7914-7918 (1989).
7. M.D. Wang, H. Yin, R. Landick, J. Gelles, and S. M. Block, “Stretching DNA with optical tweezers,” *Biophys. J.* **72**, 1335-1346 (1997).
8. M.T. Woodside, P.C. Anthony, W.M. Behnke-Parks, K. Larizadeh, D. Herschlag, and S.M. Block, “Direct measurement of the full, sequence-dependent folding landscape of a nucleic acid,” *Science*, **314**, 1001-1004 (2006).
9. Y.Z. Shi, S. Xiong, Y. Zhang, L.K. Chin, Y.-Y. Chen, J.B. Zhang, T. Zhang, W. Ser, A. Larson, L.S. Hoi, *et al.,* “Sculpting nanoparticle dynamics for single-bacteria-level screening and direct binding- efficiency measurement,” *Nat. Commun.* **9**, 815 (2018).
10. M. Righini, A.S. Zelenina, C. Girard, and R. Quidant, “Parallel and selective trapping in a patterned plasmonic landscape,” *Nat. Phys.* **3**, 477 (2007).
11. O. Jovanovic, “Photophoresis—light induced motion of particles suspended in gas,” *J. Quant. Spectrosc. RA.* **110**, 889-901 (2009).
12. A.E. Cohen and W.E. Moerner, “Method for trapping and manipulating nanoscale objects in solution,” *Appl. Phys. Lett.* **86**, 093109 (2005).
13. C. Gosse and V. Croquette, “Magnetic tweezers: micromanipulation and force measurement at the molecular level,” *Biophys. J.* **82**, 3314-3329 (2002).
14. M. Braun and F. Cichos, “Optically controlled thermophoretic trapping of single nano-objects,” *ACS Nano*, **7**, 11200-11208 (2013).
15. A.E. Cohen, “Control of nanoparticles with arbitrary two-dimensional force fields,” *Phys. Rev. Lett.* **94**, 118102 (2005).
16. A. Kumar and J. Bechhoefer, “Nanoscale virtual potentials using optical tweezers,” *Appl. Phys. Lett.* **113**, 183702 (2018).
17. R.M. Simmons, J.T. Finer, S. Chu, and J.A. Spudich, “Quantitative measurements of force and displacement using an optical trap,” *Biophys. J.* **70**, 1813-1822 (1996).
18. A. Ranaweera, and B. Bamieh, “Modelling, identification, and control of a spherical particle trapped in an optical tweezer,” *Int. J. Robust Nonlin.* **15**, 747-768 (2005).
19. A.E. Wallin, H. Ojala, E. Hffiggstrom, and R. Tuma, “Stiffer optical tweezers through real-time feedback control,” *Appl. Phys. Lett.* **92**, 224104 (2008).
20. J.A.C. Albay, G. Paneru, H.K. Pak, and Y. Jun, “Optical tweezers as a mathematically driven spatio-temporal potential generator,” *Opt. Express*, **26**, 334542 (2018).
21. Y. Jun, and J. Bechhoefer, “Virtual potentials for feedback traps,” *Phys. Rev. E*, **86**, 061106 (2012).
22. C.H. Schmitz, J.P. Spatz, and J.E. Curtis, “High-precision steering of multiple holographic optical traps,” *Opt. Express*, **13**, 8678-8685 (2005).
23. E.B. Mpemba, and D.G. Osborne, “Cool?” *Phys. Educ.* **4**, 172-175 (1969).
24. P.A. Greaney, G. Lani, G. Cicero, and J.C. Grossman, “Mpemba-like behavior in carbon nanotube resonators,” *Metall. Mater. Trans. A*, **42**, 3907-3912 (2011).
25. M. Baity-Jesi, E. Calore, A. Cruz, L.A. Fernandez, J.M. Gil-Narvion, A. Gordillo-Guerrero, D. Iniguez, A. Las- anta, A. Maiorano, E. Marinari, *et al.,* “The Mpemba effect in spin glasses is a persistent memory effect,” *Proc. Natl. Acad Sci.* **116**, 15350-15355 (2019).
26. Y.-H. Ahn, H. Kang, D.-Y. Koh, and H. Lee, “Experimental verifications of Mpemba-like behaviors of clathrate hydrates,” *Korean J. Chem. Eng.* **33**, 1903-1907 (2016).
27. M. Vynnycky, and S. Mitchell, “Evaporative cooling and the Mpemba effect,” *Heat Mass Transfer*, **46**, 881-890 (2010).
28. M. Vynnycky, and N. Maeno, “Axisymmetric natural convection-driven evaporation of hot water and the Mpemba effect,” *Int. J. Heat Mass Transfer*, **55**, 7297-7311 (2012).
29. S. Esposito, R. De Risi, and L. Somma, “Mpemba effect and phase transitions in the adiabatic cooling of water before freezing,” *Phys. A Stat. Mech. Appl.* **387**, 757-763 (2008).
30. J.I. Katz, “When hot water freezes before cold,” *Am. J. Phys.* **77**, 27-29 (2009).
31. Y. Tao, W. Zou, J. Jia, W. Li, and D. Cremer, “Different ways of hydrogen bonding in water-why does warm water freeze faster than cold water?” *J. Chem. Theory Comput.* **13**, 55-76 (2016).
32. Z. Lu, and O. Raz, “Nonequilibrium thermodynamics of the Markovian Mpemba effect and its inverse,” *Proc. Natl. Acad Sci.* **114**, 5083-5088 (2017).
33. A. Kumar, and J. Bechhoefer, “Anomalous cooling and heating in a colloidal system: Observation of the forward and inverse Mpemba effects,” In preparation.
34. Y. Jun, M. Gavrilov, and J. Bechhoefer, “High-precision test of Landauer’s principle in a feedback trap,” *Phys. Rev. Lett.* **113**, 190601 (2014).
35. M. Gavrilov, and J. Bechhoefer, “Erasure without work in an asymmetric double-well potential,” *Phys. Rev. Lett.* **117**, 200601 (2016).
36. K. Neupane, A.P. Manuel, and M.T. Woodside, “Protein folding trajectories can be described quantitatively by one-dimensional diffuison over measured energy landscapes,” *Nat. Phys.* **12**, 700-704 (2016).